Hyperfine Interactions 23(1985)211–220

HYPERFINE CHARACTERIZATION OF TIN-DOPED INDIUM SESQUIOXIDE

R.C. MERCADER, F.H. SÁNCHEZ, L.A. MENDOZA-ZÉLIS, L. TERMINIELLO, A.G. BIBILONI, C.P. MASSOLO, J. DESIMONI and A.R. LÓPEZ-GARCÍA

Departmento de Física, Facultad de Ciencias Exactas, Universidad Universidad Nacional de La Plata, Calle 49 y 115, 1900 La Plata, Argentina

Received 10 January 1985
(Revised 27 February 1985)

The hyperfine interactions at In and Sn sites of In_2O_3:Sn (ITO) were measured through time-differential perturbed angular correlations and Mössbauer spectroscopy, respectively. Polycrystalline samples prepared by co-precipitation with nominal 0.025, 1 and 5 at.% Sn were studied. They all showed the cubic bixbyite structure characteristic of In_2O_3 after annealings at 200 °C. The quadrupole interaction at In sites appears nearly independent of Sn concentration being the main result of the presence of Sn in the lattice, the gradual disappearence of the dynamic perturbation caused by after-effects. The Mössbauer data demonstrate that Sn ions are in a 4+ state with $\Delta Q = 0.60_6$ mm/s and $\delta = 0.22_6$ mm/s relative to SnO_3Ca at room temperature.

1. Introduction

Films of transparent semiconducting oxides (e.g. SnO_2:Sb, CdO:Sn, In_2O_3:Sn and Cd_2SnO_4) show a singular combination of electrical and optical properties: high concentration of nearly free electrons, U.V. absorption and high I.R. reflectance. Consequently, these oxides are of high technological importance and pose very interesting problems to the solid state physicist. They have been intensively studied by several techniques and diverse preparation methods have been developed. Nevertheless, the physical properties of these complex systems are not well understood, since they are greatly dependent on preparation methods [1].

Perhaps the most interesting of this family of oxides is the indium tin oxide (ITO), In_2O_3:Sn. Moreover, it is one of the few systems that presents naturally in its composition two elements that are good probes for two different hyperfine techniques: In for TDPAC and Sn for Mössbauer spectroscopy (ME). In spite of this advantage, a systematic investigation of its quadrupole parameters has not yet been

attempted, let alone their relation to other physical properties or dependence on the production method. Only one Mössbauer measurement on ITO films has been reported [2], but no parameter was quoted.

With this purpose in mind, we have undertaken a study of In_2O_3 doped with different concentrations of Sn, making use of the above mentioned techniques. In order to attain a good characterization of the compounds, the present research has been restricted to polycrystalline samples. We report in this paper results obtained on samples with three concentrations of Sn, namely 0.025, 1 and 5 atomic percent, which are discussed in connection to our previous measurements on undoped In_2O_3 [3].

2. Experimental

We obtained polycrystalline In_2O_3:Sn by the co-precipitation method described by Frank et al. [4]. This method assures a quick attainment of thermodynamic equilibrium due to the intimate contact of indium and tin during oxidation, but may lead to the formation of a hexagonal modification of the structure (corundum) apart from the normal cubic one described below. Solutions of $SnCl_4$ and $InCl_3$ (containing some $^{111}InCl_3$ in the samples to be analyzed by TDPAC) were mixed in adequate proportions to obtain 0.025, 1 and 5 at.% Sn. The precipitation temperature was 60 °C and the resulting gel was dried in air at 200 °C. The powders so obtained were annealed in air at temperatures ranging from 550 to 1300 °C (see table 1). X-ray diffractograms were performed on each sample after each preparation stage.

Table 1

Nominal composition and thermal treatments of the studied samples (★ indicates the experimental technique used)

Sample number	Sn concentration (at.%)	Annealings t(h) × T(°C)	X-ray	TDPAC	ME
1	0.025	15 × 200 + 10 × 1050	★	★	
2	1.0	15 × 200 + 10 × 1000	★	★	★
3	1.0	2 × 150 + 8 × 950			★
4	1.0	2 × 150 + 21 × 1040	★		★
5	5.0	15 × 200 + 16 × 530		★	
		+ 10 × 1000		★	
		+ 2 × 1300	★	★	★
6	5.0	15 × 200	★		★
		+ 9 × 560	★		★
		+ 10 × 1000	★		★
7	5.0	15 × 200	★		★
		+ 16 × 1300	★		★

The Mössbauer data, obtained with transmission geometry in constant acceleration mode, were accumulated simultaneously in two halves of 256 channels each, in a multiscaler and waveform generator developed and built at this Physics Department. A $Ca^{119m}SnO_3$ source of $\cong$ 5 mCi activity was used. A 50 μm Pd filter removed the undesirable Sn X-rays. The detector was a 2 mm thick NaI(Tl) crystal. Room temperature was kept constant within ± 1 °C at 20 °C. The two halves of the spectra were fitted independently with lorentzian curves on a parabolic baseline with a non-linear least-squares program with constraints. The velocity calibration was obtained by means of a 10 mCi ^{57}CoRh source and a 6 μm thick natural Fe foil as absorber. Velocity nonlinearity was fitted to a third degree polynomial.

The TDPAC measurements were performed using the 173–247 keV $\gamma-\gamma$ cascade following the electron-capture decay of the ^{111}In activity. The ^{111}Cd intermediate $5/2^+$ level has a lifetime of 85 ns and a quadrupole moment of $+ 0.77_{12}$ b. The angular correlation was measured using a conventional automated fast-slow coincidence setup including a 4.5×4.5 cm^2 CsF fixed detector and a 5×5 cm^2 NaI(Tl) mobile one. Time resolution was 2.4 ns (FWHM). Experimental asymmetry ratios $R(t)$ were evaluated and fitted with theoretical functions $A_2 G_2(t)$ folded with the measured time-resolution curve. Further details of the electronic equipment and data analysis can be found in ref. [5].

3. Results

The X-ray diffractograms of all the samples showed the pattern belonging to In_2O_3 with the cubic bixbyite structure (spatial group $Ia3$). None of the lines corresponding to the corundum-type modification (spatial group $R\bar{3}c$) nor the InO(OH) peaks reported by Frank et al. [4] could be observed even in samples just annealed at 200 °C. A sharpening of the lines occurred with increasing temperature of annealing due to the greater particle size. In some of the 5 at.% Sn samples, it was possible to notice two lines that denoted the presence of small quantities of SnO_2 only after annealings at 1000 °C or higher temperatures.

Figure 1 shows TDPAC spectra obtained on samples with different concentrations of tin and annealed at temperatures $\geqslant$ 1000 °C. Two static quadrupole interactions were necessary to fit the data and the resulting parameters, shown in table 2, are temperature independent between 15 and 800 K and very close to those of pure In_2O_3 [3]. These interactions can still be associated with the two non-equivalent sites of In in the crystalline structure of In_2O_3 that are in the relative population ratio of 3:1. Like undoped In_2O_3, the 0.025 at.% sample also showed a dynamic interaction that disappeared when measurements were taken at higher temperatures. This is discussed elsewhere [6].

A 5 at.% sample was also measured after an annealing at 530 °C before the 1000 °C treatment. It displayed a TDPAC spectrum clearly different from the others

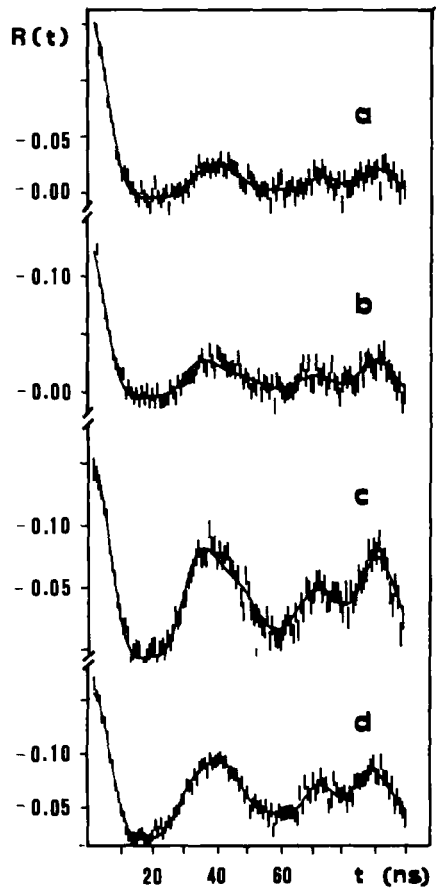

Fig. 1. TDPAC spectra at RT of In_2O_3:Sn annealed at $T \geqslant 1000$ °C containing nominally: (a) 0.0, (b) 0.025, (c) 1.0, and (d) 5.0 at.% Sn. The solid lines show the least-squares fit to the data.

Table 2

Static quadrupole parameters, $\omega_Q = eQV_{zz}2\pi/40$ h and $\eta = (V_{xx} - V_{yy})/V_{zz}$, obtained from TDPAC at room temperature, for In_2O_3:Sn after annealings at 1000 °C. The relative FWHM, δ, of a lorentzian frequency distribution around ω_Q is also quoted

at.% Sn	ω_{Q_1} (Mrad/s)	η_1	δ_1	ω_{Q_2} (Mrad/s)	η_2	δ_2
0.0	18.3_3	0.72_2	0.00_1	24.3_6	0.12_2	0.00_1
0.025	17.9_3	0.72_2	0.01_1	24.1_3	0.14_3	0.00_1
1.0	18.3_2	0.73_1	0.04_1	23.9_2	0.18_2	0.01_1
5.0	18.3_2	0.69_2	0.06_1	24.2_2	0.26_4	0.02_1

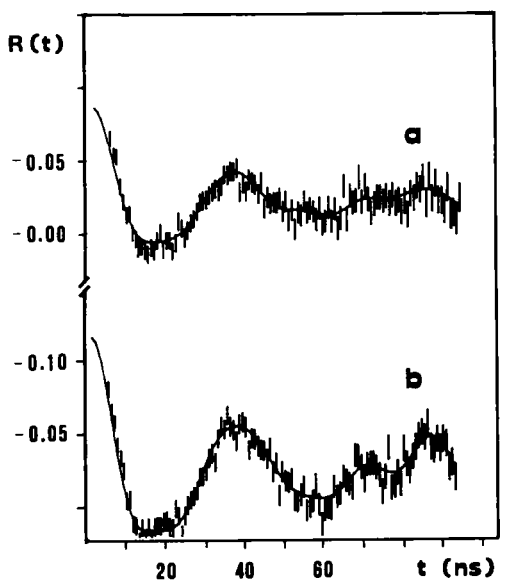

Fig. 2. TDPAC spectra at RT of In_2O_3:Sn containing nominally 5 at.% Sn annealed at: (a) 530 °C and (b) 1000 °C. The solid lines show the least-squares fit to the data.

(fig. 2) that could only be fitted allowing for a highly distributed quadrupole interaction on top of the already mentioned ones. This additional contribution accounted for 78% of the measured attenuation and was characterized by the following parameters: $\omega_Q = 20_2$ Mrad/s, $\eta = 0.5_2$, $\delta = 0.28_6$.

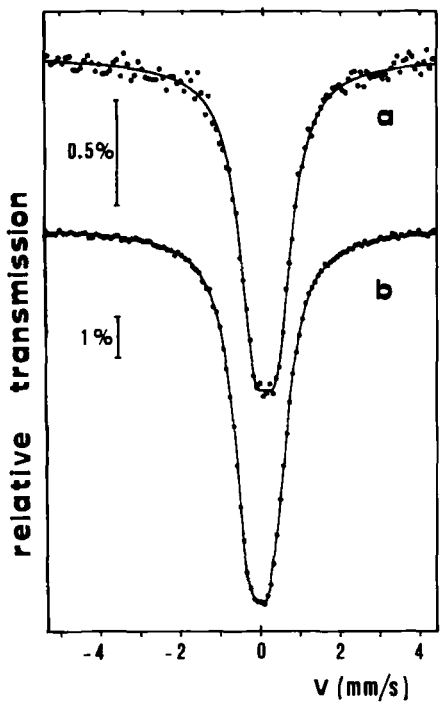

Fig. 3. Mössbauer spectra at RT of In_2O_3:Sn annealed at $T \geq 1000$ °C containing nominally: (a) 1.0 and (b) 5.0 at.% Sn. The solid lines show the least-squares fit to the data.

Figure 3 shows typical Mössbauer spectra of 1 and 5 at.% Sn samples (it was not feasible to obtain Mössbauer spectra of the 0.025 at.% Sn samples). All of the data exhibit isomer shifts characteristic of tin ions in the 4+ state and are composed of unresolved quadrupole doublets. Since the X-ray diffractograms of the 5 at.% Sn samples annealed at 1000 °C denoted the existence of SnO_2, the fittings of these samples were performed with two quadrupole interactions, one with initial fitting parameters close to those of SnO_2 and the other with values similar to those of 1 at.% Sn samples, where almost totally dissolved Sn in In_2O_3 is expected. This was con-

sidered to also be the case even for the specimens annealed at low temperature that did not show X-ray lines corresponding to SnO_2 because of the very small particle size. In should be emphasized, however, that a neat result was not expected, since the ^{119}Sn has a broad Mössbauer line and the two species, SnO_2 and tin dissolved in ITO, have apparently very similar parameters (almost identical ΔQ and isomer shifts differing at most by about 1/4 th of the natural line width). These results are shown in table 3.

Table 3

Mössbauer quadrupole parameters at ^{119}Sn in In_2O_3:Sn at room temperature. The results shown are averages over 10 measurements of 5 at.% and 8 of 1 at.% samples. The third and fourth columns are the averages of the fitted values corresponding to SnO_2. The isomer shifts are referred to $CaSnO_3$ at room temperature

at.% Sn	ΔQ (mm/s)	δ (mm/s)	$\Delta Q'$ (mm/s)	δ' (mm/s)
1.0	0.57_2	0.18_2	-	-
5.0	0.64_6	0.27_6	0.61_6	-0.02_4
Adopted values	0.60_6	0.22_6	-	-

4. Discussion

In_2O_3 crystallizes in the cubic bixbyite structure, closely related to that of CaF_2, from which it can be derived by removing orderly 1/4 of the anions and then allowing for relaxation [7]. The oxygen retains its 4-coordination, while two non-equivalent sites arise for the 6-coordinated In atoms. Twenty-five percent of indiums are occupying the centers of trigonally distorted oxygen octahedra (site b). The remaining 75% are located at the centers of more distorted octahedra of lowest symmetry (site d).

Electric field gradients arising from a pure ionic lattice account for the observed quadrupole interactions at ^{111}Cd and grant a reliable assignment of the frequencies and asymmetry parameters to the two non-equivalent In sites. Indeed, point-charge calculations, summing over 30 nearest neighbours reproduce the observed EFGs within experimental errors (see table 4). A summation over the whole lattice, using the de-Wette method, yields similar results.

In ITO, indium atoms are substituted by tin up to a small percentage that depends on the preparation method. This doping produces a broadening of the TDPAC frequency distributions and a slight increase in the value of the asymmetry parameter η_2 with concentration. In order to interpret these results, we made point-charge calcu-

Table 4

Measured and calculated V_{zz} and η of the electric field gradient at sites d and b of pure and tin-doped In_2O_3 (V_{zz} in units of 10^{17} V/cm^2)

	$(1-\gamma_\infty)V_{zz}^{d}$	η^{d}	$(1-\gamma_\infty)V_{zz}^{b}$	η^{b}	V_{zz}^{d}/V_{zz}^{b}
Pure In_2O_3 (experimental)	6.3_9	0.72_2	$8.3_{1.2}$	0.12_2	1.33
Pure In_2O_3 (calculated)	5.0	0.54	6.8	0.00	1.36
Sn^{4+} substituted at one of the 6 possible *nn* In^{3+} sites	4.9	0.56	5.6	0.61	-
Sn^{4+} substituted at one of the 6 possible *nnn* In^{3+} sites	5.3	0.62	7.7	0.09	-

lations with substitution of one Sn^{4+} ion for one In^{3+} at a site of subsequent indium neighbour shells. From the values presented in table 4 it can be seen that in spite of the crude model used (which ignores any shielding effect), the general trends are well-reproduced. With increasing Sn concentration, the probability for In probes to have one Sn^{4+} in its neighbourhood will grow. Then the measured η_2 value, resulting from the various possible η^b, will rise too. This agreement is better if preferential substitution of In at site b is proposed.

The frequencies themselves are concentration independent, but the distributions observed are mainly caused by the increasing presence of tin substituents. Frequency distributions can also originate on surface effects and, due to smaller particle sizes, these could be particularly important for samples not treated at higher temperatures. Indeed, the broadly distributed component found in the sample annealed at 530 °C can be attributed to the greater relative proportion of probes near to or at the particle surface. The X-ray diffractograms of this sample also show wider diffraction peaks that, in the framework of Bragg law [8], denote a particle diameter smaller than 10 nm. For this particle size, the relative number of bulk to surface atoms is consistent with the measured contribution of the broad frequency to the perturbation factor when atoms further than seven interatomic distances away from the surface are considered to be no longer perturbed by surface effects.

The progressive dilution of Sn in the In_2O_3 lattice causes a gradual disappearance of the time-dependent perturbation. This is originated in the after-effects produced by the electron capture in ^{111}In [6]. Its contribution lessens and finally vanishes because of the donation of the extra electrons from tin impurities to the

conduction band. This is also proof of the effective dilution of tin in the lattice. Since the measured EFG is neither dependent on tin concentration nor on the measurement temperature, it can be inferred that the conduction band has predominantly s-character. This is coherent with the schematic energy diagram proposed by Fan and Goodenough [9].

The values shown in table 3 are the averages obtained from the fittings of the Mössbauer spectra for the 1 at.% Sn samples with only one quadrupole interaction and 5 at.% Sn samples fitted against one component belonging to SnO_2 and the other to Sn in ITO. Significantly, better χ^2 values were obtained when these two quadrupole doublets were used for the theoretical fitting functions solely in the case of 5 at.% Sn samples. This was not so for 1 at.% Sn samples, where fits with two interactions gave poorer χ^2 values. However, it cannot be discarded that a very small quantity of SnO_2 may contribute to the signal.

The values of ΔQ and δ adopted for Sn dissolved in ITO are the averages over those obtained for both concentrations (see table 3). These values correspond definitively to an Sn^{4+} ion and rule out another possible charge state of the tin ion.

As already mentioned, the tin ions in ITO are substituting the indium ions of indium sesquioxide. Since TDPAC measurements reveal two clearly different quadrupole interactions, through the values of ω_Q and η, it might be expected that Mössbauer spectra also showed these two non-equivalent situations. However, since the ^{119}Sn Mössbauer transition is between levels of spins 3/2 and 1/2, the contributions of V_{zz} and η cannot be disentangled from the resulting quadrupole interaction. The quadrupole splittings corresponding to the two sites might differ at most by 23%, too small a difference to be observed through the broad ^{119}Sn Mössbauer line. Besides, the presence of SnO_2 in the samples makes the case even more difficult because of the very similar quadrupole parameters of both species. For these reasons, it is not possible to discern an eventual preferential substitution of Sn for sites b or d in the lattice.

The V_{zz} measured through ME on Sn is about five times greater than either of the two values that TDPAC yields for nominally the same site of In, taking $Q_{Cd} = 0.77$ b, $Q_{Sn} = -0.08$ b, $(1 - \gamma_\infty)_{Cd} = 30.3$ and $(1 - \gamma_\infty)_{Sn} = 11$. An explanation of this may be attempted on considering that the Sn^{4+} ion has a $\Delta Z = +1$ respective to the In ion it substitutes. This charge excess may be compensated by an increased local density of free electrons that would tend to occupy the lowest empty tin orbitals, probably hybridized to fulfill the requirements of the local symmetry, thus increasing the local EFG.

5. Conclusions

The static quadrupole parameters of ITO at indium sites are very similar to those of pure In_2O_3. Only an increase of the value of η at site b is observed.

The main consequence of the dilution of tin in the In_2O_3 lattice is its influence on the extinction of the dynamic interaction through the donation of Sn

electrons to the conduction band. The static EFGs are not altered by this augmented concentration because of the predominant s-character of these electrons.

The Mössbauer parameters of ITO at tin sites are $\delta = 0.22 \pm 0.06$ mm/s and $\Delta Q = 0.60 \pm 0.06$ mm/s, indicating a 4+ state for Sn ions. The derived EFG is greater than those measured by TDPAC, probably due to local contributions.

A bixbyite-type structure of ITO was formed at temperatures as low as 200 °C. Further annealings only contributed to enlarge the particle size. No corundum-type structure was observed for any tin concentration or annealing temperature.

Acknowledgements

The authors are grateful to CONICET and CICPBA, Argentina, and Internationales Beziehungen, Kernforschungszentrum Karlsruhe GmbH, West Germany for partial economic support. The provision of the X-ray diffractograms by CETMIC, La Plata, Argentina, and the X-ray laboratory at this Physics Department is kindly acknowledged. R.C.M., F.H.S., L.A.M.Z., A.G.B., C.P.M. and A.R.L.G. are members of Carrera del Investigador Cientifico CONICET, L.T. is a fellow of CICPBA, and J.D. is a fellow of CONICET.

References

[1] Z.M. Jarzebski, Phys. Stat. Sol. (a) 71(1982)13.
[2] H. Köstlin, R. Jost and W. Lems, Phys. Stat. Sol. (a) 29(1975)87.
[3] J. Desimoni, A.G. Bibiloni, L.A. Mendoza-Zélis, A.F. Pasquevich, F.H. Sánchez and A.R, López-Garcia, Phys. Rev. B28(1983)5739;
A.G. Bibiloni, J. Desimoni, C.P. Massolo, L.A. Mendoza-Zélis, A.F. Pasquevich, F.H. Sánchez and A.R. López-Garcia, Phys. Rev. B29(1984)1109.
[4] G. Frank, R. Olazcuaga and A. Rabenau, Inorg. Chem. 16(1977)1251.
[5] A.F. Pasquevich, F.H. Sánchez, A.G. Bibiloni, J. Desimoni and A.R. López-Garcia, Phys. Rev. B27(1983)963.
[6] A.G. Bibiloni, C.P. Massolo, J. Desimoni, L.A. Mendoza-Zélis, F.H. Sánchez, A.F. Pasquevich, L. Damonte and A.R. López-Garcia, Phys. Rev. B (to be published).
[7] M. Marezio, Acta Cryst. 20(1966)723.
[8] B.K. Vainshtein, in: *Modern Crystallography I,* Springer Series in Solid State Sciences, Vol. 15, ed. H.J. Queiser (Springer Verlag, Berlin, 1981) p. 238.
[9] J.C.C. Fan and J.B. Goodenough, J. Appl. Phys. 48(1977)3524.